



# Liquid-liquid equilibria of systems containing C1-C4 alcohols (methanol, ethanol, n-propyl alcohol, or tert-butyl alcohol), glycerol and olive oil

Larissa Madureira Pacholak do Espírito Santo, Ana Maura Novak, Maria Clara Corrêa Gomes Palma, Giulia Herbst, Luís Ricardo Shigeyuki Kanda and Fernando Augusto Pedersen Voll\*

Departamento de Engenharia Química, Universidade Federal do Paraná, Av. Cel. Francisco H. dos Santos 210, 81531-980, Curitiba, Paraná, Brasil. \*Autor for correspondente. E-mail: fernando\_voll@ufpr.br

**ABSTRACT.** This work reports experimental results and thermodynamic modeling of liquid-liquid equilibrium of systems containing alcohols with 1 to 4 carbons, glycerol, and olive oil. Experiments were conducted at 35°C and atmospheric pressure. UNIQUAC model was used to calculate the phase equilibria and fitted well the experimental data with root mean square deviations below 1 wt.% for all studied systems. Additionally, consistency was observed between the calculated and experimental binodal curves. The results obtained here showed that the miscibility region of ternary systems increases with the increased number of carbons in the alcohol. By studying the behavior of ternary systems, glycerolysis reactions in the presence of solvents, aiming to produce diacylglycerol-rich oils, could be designed to work in the single-phase region, enhancing product yields. However, side reactions could lead to the production of fatty acid alkyl esters, due to the presence of alcohols. Aspen Plus® v. 12.1 was used to assess whether the formation of diacylglycerols (DAG) or esters was thermodynamically favorable, indicating the possibility of using t-butanol as a solvent to enhance DAG yield.

**Keywords:** Olive oil; Glycerol; Alcohols; Liquid-liquid Equilibrium.

Received on October 22, 2024.

Accepted on November 12, 2025.

## Introduction

The constant changes in dietary habits and living standards have significantly contributed to a rising global prevalence of lifestyle-related diseases, such as obesity and cardiovascular diseases. These health issues are often associated with excessive intake of dietary fats, particularly saturated and trans fats. As a response to these challenges, there has been an increased interest in functional oils that may offer health benefits beyond basic nutrition (Ke et al., 2024; Xie et al., 2024).

One of such functional oil is diacylglycerol (DAG). This unique lipid naturally occurs in various oils in low fractions and is composed of a glycerol backbone bonded to two fatty acid molecules. Unlike traditional triacylglycerols, DAG is believed to have several health advantages (Lo et al., 2008). Research suggests that DAG may promote weight management and help reduce fat accumulation in the body. Additionally, its structure may influence metabolic processes in a way that supports cardiovascular health. As consumers become more health-conscious, the exploration and incorporation of functional oils like DAG into diets could play a significant role in leading to improved overall well-being (Ke et al., 2024; Zhou et al., 2022).

Liquid oils can be transformed into structural fats via enzymatic glycerolysis, producing monoacylglycerols (MAGs) and diacylglycerols (DAGs), widely used as emulsifiers in the food industry. Moreover, DAG oil has been commercialized due to its well-documented health benefits when consumed instead of triacylglycerols (TAGs) (Nicholson & Marangoni, 2022).

Glycerolysis is a significant chemical reaction involving the transesterification of glycerol with triacylglycerols, such as those found in olive oil, to produce mono- and diacylglycerols (Chen et al., 2021). Due to their emulsifying properties, these compounds have a wide range of applications in the food, pharmaceutical, and cosmetic industries. However, one of the challenges in glycerolysis reactions is the inherent immiscibility between hydrophobic olive oil and hydrophilic glycerol (Fetes et al., 2013). To enhance the degree of contact between the TAGs content in olive oil and glycerol, the addition of solvents is a suitable

alternative to improve the contact between the two liquid phases thus increasing the solubility of both phases, aligned with parameters such as agitation, and reaction temperature (Damstrup et al., 2005, Damstrup et al., 2006; Kumoro, 2012; McNeill et al., 1991; Naik et al., 2014; Rabiah et al., 2021; Singh & Mukhopadhyay, 2016; Zhong et al., 2009).

Cabral et al. (2018) studied the liquid-liquid phase equilibrium of hydrolyzed olive oil, composed of TAGs, DAGs, MAGs, and free fatty acids, with ethanol and water. The results of subsequent analysis of the oil's oxidative stability obtained from the liquid phases show the potentiality of liquid-liquid extraction as a suitable procedure for olive oil enrichment in diacylglycerol. Moreover, Soares et al (2018) investigated the system of glycerolized olive oil, and glycerol using ethanol to enhance solubility between the components indicating the feasibility of diacylglycerol separation from other triacylglycerols and free fatty acids through liquid-liquid phase separation. Further, Oliveira et al. (2022) analyzed thermodynamic modeling of liquid-liquid equilibrium of systems containing mono-, di- and triacylglycerols from olive oil, glycerol, and isopropanol. Both works applied the UNIQUAC model to describe phase equilibria, which was well-fitted to experimental data.

In this way, using alcohols as solvents has been explored to enhance the miscibility between these two components, thereby improving the reaction efficiency and product yield. Alcohols, such as methanol, ethanol, and isopropanol, act as co-solvents that reduce the interfacial tension, promoting better mixing and contact between glycerol and olive oil (Jin et al., 2019). This approach can lead to higher yields of the desired mono- and diglycerides, making the process more efficient and economically viable (Li et al., 2023). Understanding the role of alcohols in enhancing miscibility and optimizing the glycerolysis reaction is crucial for advancing industrial applications and achieving sustainable production processes (Jin et al., 2019; Sandid et al., 2024). Thus, the present research aimed to fit UNIQUAC's binary interaction parameters using data for methanol, ethanol, isopropyl alcohol, and tert-butyl alcohol and check whether these parameters can describe the system containing propanol. The UNIQUAC model was used to describe the liquid-liquid equilibrium because, compared to the NRTL model, it has the advantage of incorporating structural parameters related to the size and shape of molecules, such as volumes and surface areas. This is particularly relevant in systems with molecules of very distinct sizes and shapes, as is the case with triglycerides in contrast to C1-C4 alcohols and glycerol.

## Material and methods

### Materials

Extra-virgin olive oil (Andorinha) was acquired at a local market and used in the experimental section of this work. For the extractions performed as part of the analytical technique, deionized water prepared in our facilities was used. Table 1 lists the other chemicals, used as supplied by the manufacturers, without previous purification.

**Table 1.** Chemicals used in the experimental section.

Compound	CAS Number	Molecular structure	Supplier	Molar Mass g mol <sup>-1</sup>	Min. Purity (mass fraction)
Glycerol	56-81-5	C3H8O3	ACS Cientifica	92.09	0.995
Methanol	67-56-1	CH4O	Neon	32.02	0.998
Ethanol	64-17-5	C2H6O	Neon	46.07	0.995
n-Propanol	71-23-8	C3H8O	Neon	60.09	0.998
tert-Butanol	75-65-0	C4H10O	ACS Cientifica	74.12	0.990
Hexane	110-54-3	C6H14	Neon	86.18	0.990

### Liquid-Liquid (LLE) experimental data

LLE experimental data comprising binodal curves and tie lines were determined at 35°C for the ternary systems (methanol, ethanol, n-propanol, or t-butanol) + glycerol + olive oil. Two different methodologies were employed here, both following those used by Oliveira et al. (2022). In short, the binodal curves were determined using the cloud-point methodology, in which known amounts of each component are fed into low-pressure, jacketed, glass equilibrium cells until a second liquid phase is detected visually. The temperature was kept at 35°C using a thermostatic bath (Vivo, model RT4) coupled to the equilibrium cells.

For the determination of tie lines, the desired compositions were placed inside vials and the ternary mixtures were subjected to a thorough agitation for 1 h using an agitation plate (Ika, model C-MAG HS 7). During this period, the vials were placed inside the glass equilibrium cells, so that the temperature could be controlled at 35°C. After that, the vials were placed inside an oven at 35°C for a sufficient time, allowing phase split.

After the formation of two translucent liquid phases with a well-defined interface, one sample of each phase was carefully collected in test tubes and placed inside an oven (Ethik technology, model 440-1D) at 60°C for at least 24 h. This step is aimed at the alcohol removal and the exact amount can be determined by mass differences of the samples before and after this procedure.

After that, the samples containing only olive oil and glycerol were subjected to another extraction technique, also presented by Oliveira et al. (2022), in which approximately 2 mL of hexane and 2 mL of water are added to the test tubes. The extraction solvents are vigorously mixed and the test tubes are left to rest allowing another phase separation, resulting in an aqueous phase and an organic phase. A sample of each phase is collected and placed in different test tubes, which are taken to ovens for solvent removal. The organic phase remained at 60°C for at least 48 h, while the aqueous remained at 90°C for at least 96 h. When this procedure is performed, the residual masses left in the test tubes after solvent removal correspond to masses of olive oil and glycerol, respectively, in organic and aqueous phases. Thus, the test tubes have to be weighed empty and with samples, before and after solvent removal, so that the masses can be determined and, eventually, the concentrations and the mass fractions of each component. This methodology was validated using synthetic samples with known compositions, allowing the computation of the standard uncertainties reported as a footnote in each table.

### LLE thermodynamic modeling

Experimental data obtained in this work were used to estimate the binary interaction parameters of the UNIQUAC model (Santos et al., 2018) according to the methodology described by Soares et al (2018) and Oliveira et al. (2022). The Scilab software was utilized for liquid-liquid equilibrium calculations through Gibbs free energy minimization and for the estimation of model parameters.

### Reaction simulation using Aspen Plus®

The general purpose of adding a solvent in these reactions is to facilitate the contact between the reactants. However, the presence of alcohols and TAG in the reaction might lead to transesterification, with the formation of fatty acid alkyl esters. To evaluate if the solvent's presence leads to undesired side reactions, a simulation was performed using the software Aspen Plus and the model RGIBBS. This model of equipment is a reactor that minimizes Gibbs Energy and indicates whether the formation of a determined compound is thermodynamically favorable.

The first step of the simulation is to define the components present in the process. Therefore, all the possible components were inserted as listed in Table 2. They were inserted in the simulation as 'conventional' and the column Component ID refers to the name that appears in the tables generated by the software. It is important to mention that for TAG, DAG, and MAG, a single acylglycerol of each type was defined in the simulations, to simplify the list of components. The chosen acylglycerols (triolein, diolein, and monoolein) are derived from oleic acid, the major compound in the fatty acid profile of olive oil. This strategy also allowed defining a single ester to be tracked for each alcohol used.

Table 2. List of components defined in the Aspen Plus® simulation.

Component ID	Component sanname	Alias	CAS number
TAG	Triolein	C57H104O6	122-32-7
DAG	Diolein	C39H72O5	2465-32-9
MAG	Monoolein	C21H40O4	111-03-5
GLY	Glycerol	C3H8O3	56-81-5
METOH	Methanol	CH4O	67-56-1
ETOH	Ethanol	C2H6O-2	64-17-5
IPROPOH	Isopropyl-alcohol	C3H8O-2	67-63-0
NPROPOH	1-propanol	C3H8O-1	71-23-8
TBUTOH	Tert-butyl-alcohol	C4H10O-4	75-65-0
METES	Methyl-oleate	C19H36O2	112-62-9
ETES	Ethyl-oleate	C20H38O2-N1	111-62-6
IPROPES	Isopropyl-oleate	C21H40O2-D1	112-11-8
NPROPES	Propyl-oleate	C21H40O2	111-59-1
TBUTES	Butyl-oleate	C22H42O2-N5	142-77-8

A thermodynamic model was chosen to start a simulation. Since UNIQUAC was used to fit the experimental data, the same model was used for simulations. The reactor conditions were varied in terms of temperature, ranging from 35°C to 80°C, while the pressure was kept constant at 1 atm. Calculation options for this

equipment were selected to calculate both phase equilibrium and chemical equilibrium. It was also specified that the number of fluid phases was two and the vapor phase was not taken into account for this calculation. The feed stream was also varied, so as to evaluate the effect of each alcohol on the product stream. The configurations set as input for the RGIBBS also required the estimation of some physical properties, which was possible by setting the software to calculate the bonds for all the components in the simulation.

## Results and discussion

### Determination of UNIQUAC model parameters

Twenty-seven experimental tie lines, which comprised 162 experimental mass fraction values, were used for estimating 22 binary interaction parameters of the UNIQUAC model. The  $r$  and  $q$  parameters for the studied system are presented in Table 3.

**Table 3.** UNIQUAC  $r$  and  $q$  parameters for the components studied.

Component	$r$	$q$
Olive oil*	38.5601	31.2856
Glycerol**	4.7957	4.9080
Methanol**	1.9011	2.0480
Ethanol**	2.5755	2.5880
<i>n</i> -propanol**	3.2499	3.1280
Isopropanol**	3.2491	3.1240
Tert-butanol**	3.9228	3.7440

\*Obtained from Soares et al (2018);\*\*Calculated from UNIFAC groups.

The binary interaction parameters  $A_{ij}$  and  $A_{ji}$  for the different ternary systems are listed in Table 4. Only one pair of parameters was estimated for the interactions between olive oil and glycerol to describe all the systems studied.

**Table 4.**  $A_{ij}$  (K) and  $A_{ji}$  (K) parameters for olive oil (1), glycerol (2), methanol (3), ethanol (4), *n*-propanol (5), isopropanol (6) and tert-butanol (7).

Pair i-j	$A_{ij}$	$A_{ji}$
1-2	179.87	43.323
1-3	325.09	-36.250
1-4	216.29	-38.695
1-5	203.48	-64.295
1-6	212.85	-67.977
1-7	159.27	-64.332
2-3	-132.50	40.777
2-4	-15.042	13.926
2-5	95.671	6.3973
2-6	87.588	19.452
2-7	134.00	-5.8486

### Experimental and calculated ELL data

The measured binodal curves of the systems studied here are presented in Table 5. The overall compositions used for obtaining the experimental tie lines of the ternary systems found in Table 6.

**Table 5.** Experimental binodal curves of the systems olive oil (1) + glycerol (2) + methanol (3), or ethanol (4), *n*-propanol (5), or tert-butanol (7), at 35°C and 91.2 kPa, in mass percentage (100 $w_i$ ).

100 $w_1$	100 $w_2$	100 $w_3$	100 $w_1$	100 $w_2$	100 $w_4$	100 $w_1$	100 $w_2$	100 $w_5$	100 $w_1$	100 $w_2$	100 $w_7$
0.36	79.75	19.89	0.20	99.80	0.00	0.43	99.57	0.00	0.29	99.71	0.00
0.34	58.53	41.13	0.70	89.28	10.02	0.50	66.43	33.07	0.13	81.50	18.37
0.35	36.55	63.10	0.10	43.95	55.95	0.51	49.00	50.49	0.12	69.07	30.81
0.31	17.57	82.12	2.88	5.78	91.34	1.64	29.93	68.43	0.12	55.27	44.61
0.28	4.82	94.90	4.55	0.00	95.45	3.07	22.91	74.02	0.97	40.47	58.56
			81.26	0.00	18.74	4.30	19.05	76.65	2.27	31.54	66.19
			90.17	0.05	9.78	5.07	17.51	77.42	4.50	25.80	69.70
			99.40	0.60	0.00	7.00	14.30	78.70	6.85	21.98	71.17
						8.90	12.05	79.05	10.31	18.51	71.18
						13.47	9.65	76.88	15.91	15.18	68.91
						16.68	8.49	74.83	17.06	15.03	67.91
						22.62	6.56	70.82	21.82	13.29	64.89

					36.76	2.73	60.51	27.28	11.65	61.07
					52.98	0.23	46.79	32.82	10.15	57.03
					68.63	0.72	30.65	38.07	8.88	53.05
					84.33	0.46	15.21	45.27	6.51	48.22
					99.50	0.50	0.00	50.83	5.35	43.82
								55.71	4.39	39.90
								61.77	3.38	34.85
								66.64	2.61	30.75
								72.18	1.85	25.97
								78.52	1.10	20.38
								90.24	0.53	9.23
								94.67	0.48	4.85
								99.80	0.20	0.00

Standard uncertainties  $u_{\text{areu}}(w) = 0.80 \text{ wt.\%}$ ,  $u(T) = 0.5^\circ\text{C}$  and  $u(p) = 0.3 \text{ kPa}$ .

**Table 6.** Overall compositions for the tie lines of the system Olive oil (1) + glycerol (2) + methanol (3), or ethanol (4), or n-propanol (5), or tert-butanol (7), in mass percentage (100w<sub>i</sub>).

Tie line	100w <sub>1</sub>	100w <sub>2</sub>	100w <sub>3</sub>	100w <sub>1</sub>	100w <sub>2</sub>	100w <sub>4</sub>	100w <sub>1</sub>	100w <sub>2</sub>	100w <sub>5</sub>	100w <sub>1</sub>	100w <sub>2</sub>	100w <sub>7</sub>
1	47.49	42.49	10.02	47.14	42.46	10.40	44.93	44.90	10.17	44.45	45.43	10.12
2	42.34	32.58	25.08	44.38	35.88	19.76	40.17	40.01	19.82	41.71	37.68	20.61
3	39.89	25.11	35.00	42.10	28.35	29.55	35.08	34.97	29.95	39.85	30.32	29.83
4	44.81	9.95	45.24	45.30	10.13	44.57	34.85	25.14	40.01	39.08	22.19	38.73
5	50.11	0.00	49.89	42.92	18.21	38.87	34.89	16.02	49.09	39.05	15.08	45.87
6							35.07	7.60	57.33			

Standard uncertainties  $u$  are  $u(100w) = 0.05 \text{ wt.\%}$

Tables 7, 8, 9, 10 and 11 present the experimental and calculated (using the UNIQUAC model) compositions of each tie line.

**Table 7.** Experimental data and calculated values (UNIQUAC) of the liquid-liquid equilibrium of the system olive oil (1) + glycerol (2) + methanol (3), at 35°C and 91.2 kPa, in mass percentage (100w<sub>i</sub>).

TieLine	Olive oil-richphase			Glycerol-richphase		
	100w <sub>1</sub>	100w <sub>2</sub>	100w <sub>3</sub>	100w <sub>1</sub>	100w <sub>2</sub>	100w <sub>3</sub>
Experimental data						
1	98.62	0.11	1.27	0.91	81.70	17.39
2	96.98	0.49	2.53	0.23	57.56	42.21
3	96.40	0.37	3.23	0.41	42.76	56.83
4	92.37	0.64	6.99	0.54	19.41	80.05
5	93.44	0.00	6.56	0.85	0.00	99.15
UNIQUAC model						
1	98.84	0.47	0.69	0.00	83.05	16.95
2	97.66	0.26	2.08	0.00	57.53	42.47
3	96.74	0.16	3.10	0.01	43.00	56.99
4	94.82	0.05	5.13	0.07	19.59	80.34
5	93.14	0.00	6.86	0.56	0.00	99.44

Experimental standard uncertainties  $u$  are  $u(100w_1) = 3.1 \text{ wt.\%}$ ,  $u(100w_2) = 1.8 \text{ wt.\%}$ ,  $u(100w_3) = 1.9 \text{ wt.\%}$ ,  $u(T) = 0.5^\circ\text{C}$  and  $u(p) = 0.3 \text{ kPa}$ .

**Table 8.** Experimental data and calculated values (UNIQUAC) of the liquid-liquid equilibrium of the system olive oil (1) + glycerol (2) + ethanol (4), at 35°C and 91.2 kPa, in mass percentage (100w<sub>i</sub>).

TieLine	Olive oil-richphase			Glycerol-richphase		
	100w <sub>1</sub>	100w <sub>2</sub>	100w <sub>4</sub>	100w <sub>1</sub>	100w <sub>2</sub>	100w <sub>4</sub>
Experimental data						
1	97.30	0.17	2.53	0.81	82.21	16.98
2	95.59	0.28	4.13	0.35	67.15	32.50
3	94.28	0.33	5.39	0.30	51.31	48.39
4	91.91	0.76	7.33	0.51	33.75	65.74
5	89.93	0.65	9.42	1.45	19.65	78.90
UNIQUAC model						
1	97.58	0.59	1.82	0.00	82.23	17.77
2	95.86	0.55	3.59	0.00	66.94	33.06
3	93.87	0.49	5.64	0.01	51.53	48.46
4	91.24	0.40	8.35	0.09	34.51	65.40
5	88.56	0.30	11.14	0.45	20.55	79.00

Experimental standard uncertainties  $u_{\text{areu}}(100w_1) = 3.1 \text{ wt.\%}$ ,  $u(100w_2) = 1.8 \text{ wt.\%}$ ,  $u(100w_4) = 1.9 \text{ wt.\%}$ ,  $u(T) = 0.5^\circ\text{C}$  and  $u(p) = 0.3 \text{ kPa}$ .

**Table 9.** Experimental data and calculated values (UNIQUAC) of the liquid-liquid equilibrium of the system olive oil (1) + glycerol (2) + n-propanol (5), at 35°C and 91.2 kPa, in mass percentage (100w<sub>i</sub>).

TieLine	Olive oil-richphase			Glycerol-richphase		
	100w <sub>1</sub>	100w <sub>2</sub>	100w <sub>5</sub>	100w <sub>1</sub>	100w <sub>2</sub>	100w <sub>5</sub>
Experimental data						
1	94.50	0.18	5.32	0.43	84.33	15.24
2	91.36	0.22	8.42	0.72	70.17	29.11
3	89.27	0.33	10.40	0.17	57.06	42.77
4	86.31	0.42	13.27	0.20	41.55	58.25
5	83.22	0.37	16.41	1.87	26.69	71.44
6	74.48	0.67	24.85	9.96	11.39	78.65
UNIQUAC model						
1	94.67	0.82	4.51	0.00	83.91	16.08
2	91.25	0.96	7.79	0.00	70.06	29.94
3	88.45	1.07	10.48	0.03	56.93	43.04
4	85.24	1.16	13.61	0.28	41.28	58.44
5	81.44	1.20	17.36	1.69	26.48	71.83
6	74.49	1.12	24.39	9.22	11.06	79.73

Experimental standard uncertainties  $u_{areu}(100w_i) = 3.1$  wt.%,  $u(100w_2) = 1.8$  wt.%,  $u(100w_5) = 1.9$  wt.%,  $u(T) = 0.5^\circ\text{C}$  and  $u(p) = 0.3$  kPa.

**Table 10.** Experimental data and calculated values (UNIQUAC) of the liquid-liquid equilibrium of the system olive oil (1) + glycerol (2) + isopropanol (6), at 35°C and 91.2 kPa, in mass percentage (100w<sub>i</sub>).

TieLine	Olive oil-richphase			Glycerol-richphase		
	100w <sub>1</sub>	100w <sub>2</sub>	100w <sub>6</sub>	100w <sub>1</sub>	100w <sub>2</sub>	100w <sub>6</sub>
Experimental data*						
1	93.26	1.69	5.05	0.78	85.84	13.39
2	91.11	0.85	8.04	0.19	72.10	27.71
3	89.45	0.66	9.88	0.78	57.38	41.84
4	86.08	1.12	12.80	0.65	42.59	56.76
5	82.37	1.13	16.50	2.22	26.47	71.31
6	76.63	0.84	22.53	6.25	14.47	79.29
UNIQUAC model						
1	95.13	0.80	4.07	0.00	85.75	14.25
2	91.53	0.95	7.51	0.00	71.82	28.18
3	88.56	1.07	10.37	0.03	58.03	41.94
4	85.63	1.16	13.22	0.24	42.97	56.79
5	81.87	1.21	16.93	1.76	26.70	71.54
6	77.11	1.16	21.73	7.11	13.91	78.98

\*Experimental data from Oliveira et al. (2022).

**Table 11.** Experimental data and calculated values (UNIQUAC) of the liquid-liquid equilibrium of the system olive oil (1) + glycerol (2) + tert-butanol (7), at 35°C and 91.2 kPa, in mass percentage (100w<sub>i</sub>).

TieLine	Olive oil-richphase			Glycerol-richphase		
	100w <sub>1</sub>	100w <sub>2</sub>	100w <sub>7</sub>	100w <sub>1</sub>	100w <sub>2</sub>	100w <sub>7</sub>
Experimental data						
1	91.33	0.41	8.26	0.99	89.59	9.42
2	85.86	0.66	13.48	0.13	74.60	25.27
3	80.84	1.25	17.91	0.58	58.42	41.00
4	75.39	1.91	22.70	1.17	42.94	55.89
5	72.40	2.45	25.15	3.33	29.74	66.93
UNIQUAC model						
1	92.73	0.95	6.32	0.00	88.67	11.33
2	85.78	1.37	12.85	0.00	74.06	25.94
3	80.86	1.71	17.42	0.04	58.32	41.64
4	76.88	1.99	21.13	0.43	42.46	57.10
5	72.71	2.24	25.04	1.97	30.36	67.66

Experimental standard uncertainties  $u_{areu}(100w_i) = 3.1$  wt.%,  $u(100w_2) = 1.8$  wt.%,  $u(100w_7) = 1.9$  wt.%,  $u(T) = 0.5^\circ\text{C}$  and  $u(p) = 0.3$  kPa.

Figures 1, 2, 3, 4 and 5 illustrate the data from Tables 5, 6, 7, 8, 9, 10 and 11 in ternary diagrams. In all ternary systems, the slopes of tie lines within each system present monotonic changes, indicating the good coherence of tie lines presented in this work. Moreover, the slopes of the tie lines also indicate that all studied alcohols have a greater affinity for glycerol than olive oil (or, to be more specific, with the triacylglycerols that form olive oil). However, for the homologous series of alcohols used here, longer chains represent increased

non-polar characters, and thus the immiscibility region decreases as a result of the higher affinity of longer-chain alcohols for triacylglycerols, which are non-polar molecules.

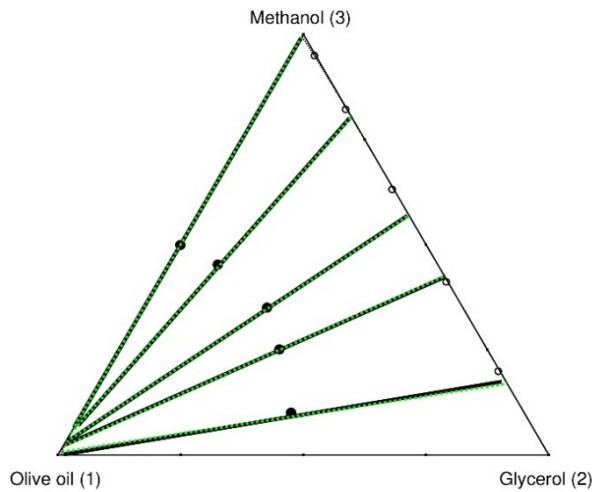


**Figure 1.** Liquid-liquid equilibrium for the ternary system olive oil (1) + glycerol (4) + methanol (3) at 35°C and 91.2 kPa. Full circles: Experimental overall composition, open circles: experimental binodal, black solid lines: experimental tie lines, green dashed lines: calculated tie lines, black dotted line: calculated binodal.

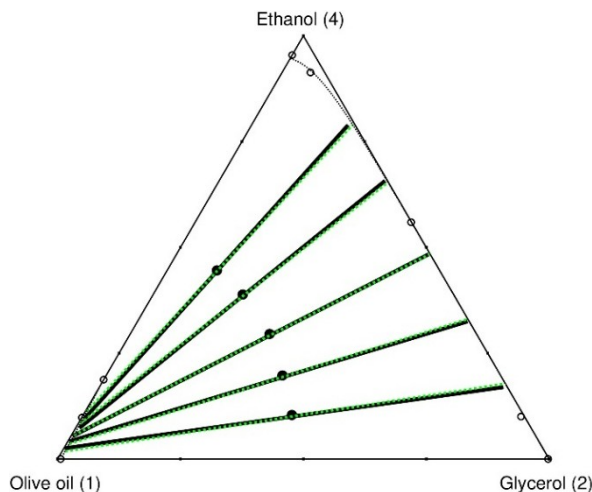


**Figure 2.** Liquid-liquid equilibrium for the ternary system olive oil (1) + glycerol (4) + ethanol (4) at 35°C and 91.2 kPa. Full circles: Experimental overall composition, open circles: experimental binodal, black solid lines: experimental tie lines, green dashed lines: calculated tie lines, black dotted line: calculated binodal.

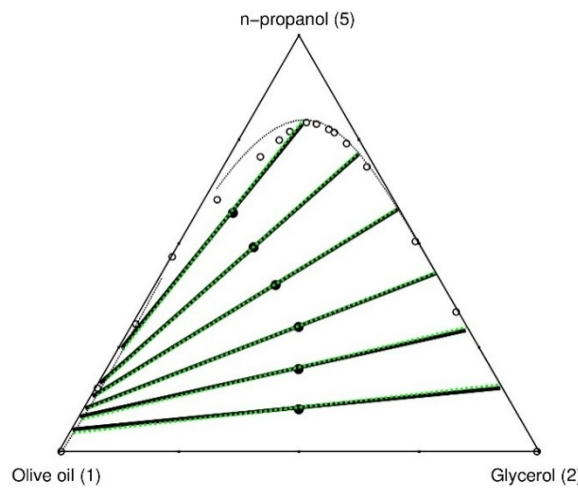


**Figure 3.** Liquid-liquid equilibrium for the ternary system olive oil (1) + glycerol (4) + n-propanol (5) at 35°C and 91.2 kPa. Full circles: Experimental overall composition, open circles: experimental binodal, black solid lines: experimental tie lines, green dashed lines: calculated tie lines, black dotted line: calculated binodal.

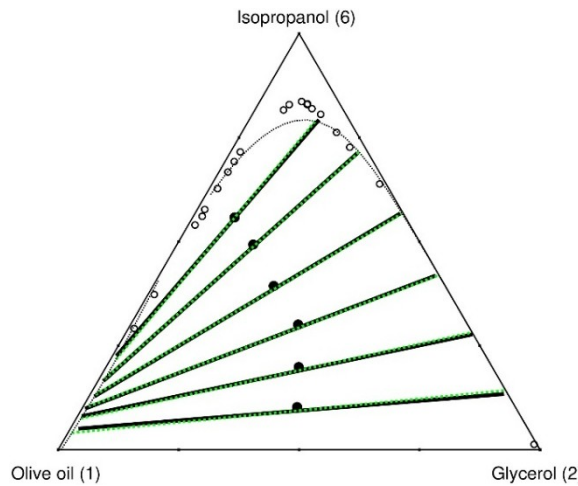


**Figure 4.** Liquid-liquid equilibrium for the ternary system olive oil (1) + glycerol (4) + isopropanol (6) at 35°C and 91.2 kPa. Full circles: Experimental overall composition, open circles: experimental binodal, black solid lines: experimental tie lines, green dashed lines: calculated tie lines, black dotted line: calculated binodal. Experimental data from Oliveira et al. (2022).

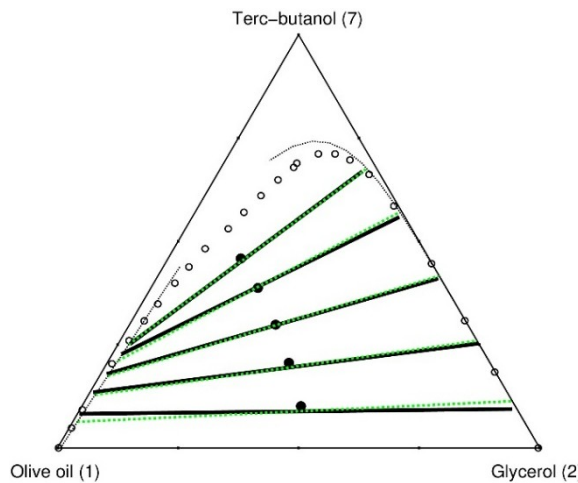


**Figure 5.** Liquid-liquid equilibrium for the ternary system olive oil (1) + glycerol (4) + tert-butanol (5) at 35°C and 91.2 kPa. Full circles: Experimental overall composition, open circles: experimental binodal, black solid lines: experimental tie lines, green dashed lines: calculated tie lines, black dotted line: calculated binodal.

The *root-mean-square deviations (rmsd)* between experimental and calculated data for all studied systems are presented in Table 12.

**Table 12.** Root-mean-square deviations between experimental and calculated tie lines for ternary systems containing olive oil, glycerol, and a C1-C4 alcohol.

Alcohol	rmsd (wt.%)
Methanol	0.7
Ethanol	0.7
n-propanol	0.6
Isopropanol	0.7
Tert-butanol	0.6

The low *rmsd* values, as well as the good agreement observed in Figures 1, 2, 3, 4 and 5, show that the UNIQUAC model was adequate to describe the phase equilibria for different ternary systems even though a single binary interaction parameter pair was considered for olive oil and glycerol.

Although the experimental binodal curves were not directly used in parameter estimation, there was good agreement between the data predicted by the UNIQUAC model and the experimental data. This is due to the good distribution of the overall compositions used in the experiments and the calculations of phase equilibrium at some points within the miscible region defined by the experimental binodal curve. If the adjusted parameters indicate a phase separation for a global composition in the known miscible region, the

objective function is automatically penalized since the compositions of the tie line will differ from the overall composition. Without this strategy, the model could erroneously predict immiscibility for certain concentration ranges in mixtures of olive oil with (n/iso)-propanol and tert-butanol since the trends of the experimental tie lines would align with this behavior. The points from the miscible region used in the objective function penalization are presented in Table 13.

**Table 13.** Points where the mixture of olive oil (1) + glycerol (2) + alcohol (5-7) was considered miscible, during the parameter estimation process.

Point	100w <sub>1</sub>	100w <sub>2</sub>	100w <sub>i</sub>	<i>i</i>
1	23	3	74	<i>n</i> -propanol
2	23	2	75	Isopropanol
3	41	4	55	Tert-butanol

With the aforementioned strategy, in addition to the proposed model adequately predicting phase separation in the immiscible region, it was also possible to precisely predict whether a separation should occur. In many situations, such as defining reaction conditions where potential reagents must be completely miscible, ensuring miscibility at certain concentrations becomes more important than knowing the composition of different phases in an immiscible region.

#### Aspen Plus® reaction simulation

In a previous analysis, Oliveira et al. (2022) performed glycerolysis reactions to obtain a glycerolized olive oil for the LLE study. Such reactions were performed at 80°C, using a Novozym435 lipase manufactured by Novozymes, with the following amounts of reactants: 150 g of olive oil, 50 g of glycerol, and 2.25 g of enzyme (1.5 wt.% the amount of olive oil). In the present study, all the simulations were performed using the amounts mentioned above of olive oil and glycerol. It is important to mention that the catalyst was not implemented in the simulation.

Reactor feed compositions were varied to determine the effect of different solvents on the reactor effluent (products formed) and the results are presented in Table 14. At this step, the presence of each solvent was tested independently, with the amount set at 800 g. The amount of solvent was chosen so that the composition of reaction media (alcohol + olive oil + glycerol), would lie in the single-phase region, at least for the longer-chain alcohols, which present a wider single-phase region compared to methanol and ethanol.

Since the main product of interest is DAG, when considering only the simulation of solvent-free reactions, performed at 35 and 80°C, the lower temperature resulted in a slightly higher amount of DAG. Moreover, the results obtained when different alcohols were tested indicated that using tert-butanol as solvent allowed DAG mole flows in reactor effluent to be as high as those obtained in solvent-free media. When ester formation is evaluated in the reactor effluent, the formation of esters is thermodynamically favored when shorter-chain alcohols are used as a solvent. Fatty acid alkyl ester mole flows obtained were 0.51 kmol h<sup>-1</sup> (methyl), 0.43 kmol h<sup>-1</sup> (ethyl), 0.09 kmol h<sup>-1</sup> (n-propyl), and values below 1E-4 for alkyl esters derived from isopropanol and tert-butanol.

**Table 14.** Composition of reactor effluents for different feed compositions, simulated using Aspen Plus®

Stream	T (°C)	Solvent	Mole Flow (kmol h <sup>-1</sup> )			
			TAG	DAG	MAG	Glycerol
Feed	35	<sup>a</sup>	0.1694	0	0	0.5429
Product	35	Free	2.73E-6	0.2504	0.0074	0.4545
Product	80	Free	1.51E-5	0.2430	0.0221	0.4472
Product	80	Methanol	1.07E-11	4.20E-5	0.0008	0.7115
Product	80	Ethanol	1.91E-7	0.0279	0.0178	0.6666
Product	80	n-Propanol	7.90E-6	0.1945	0.0217	0.4962
Product	80	isopropanol	2.37E-4	0.2423	0.0229	0.4469
Product	80	tert-butanol	1.25E-5	0.2430	0.0220	0.4472

<sup>a</sup> Feed stream solvent is the same as present in each product stream.

The previous results indicated tert-butanol might be an interesting solvent for glycerolysis since this alcohol has a wider single-phase region, which could increase the possibilities of feed stream composition. Moreover, from a thermodynamic standpoint, using this alcohol as a solvent can be interesting to avoid the transesterification of TAG during the glycerolysis, since this side reaction would lead to the formation of undesired compounds.

Thus, two sensitivity analyses were implemented using tert-butanol as a solvent, to evaluate the effects of tert-butanol mole flow in the feed (from 10 g to 800 g) and of reaction temperature (from 35°C to 80°C) on the composition of the reactor effluent. The results, in Figure 6(A) and Figure 6(B), indicated small differences in the mole flows of all components, for both sensitivity analyses. Nonetheless, when the amount of solvent is increased, DAG formation slightly increases. When the temperature increases, thermodynamics does not favor the formation of DAG, but rather the formation of MAG.

Since the software Aspen Plus® also allowed checking the number of phases of the reactor effluent as predicted by the UNIQUAC model, when the first sensitivity analysis was performed, the phase split was monitored. These results are presented in Figure 7(A) and Figure 7(B). In this sense, L1 is the first liquid, which is the acylglycerols-rich, light-phase, while L2 is the second liquid, which is the glycerol-rich, heavy-phase. The increment in the amount of tert-butanol added to the feed allowed us to observe that when at least 300 g of this component is present in the feed, a single liquid phase is predicted by the software for the reactor effluent. Furthermore, Figure 7(B) indicates slight increases in fatty acid tert-butyl ester with increased amounts of tert-butanol added to feed. In conclusion, since the equipment model implemented in the simulations using Aspen Plus® indicated that the formation of DAG is thermodynamically favorable, while the opposite is verified for fatty acid tert-butyl esters, the use of tert-butanol as a solvent for glycerolysis reactions should be considered.

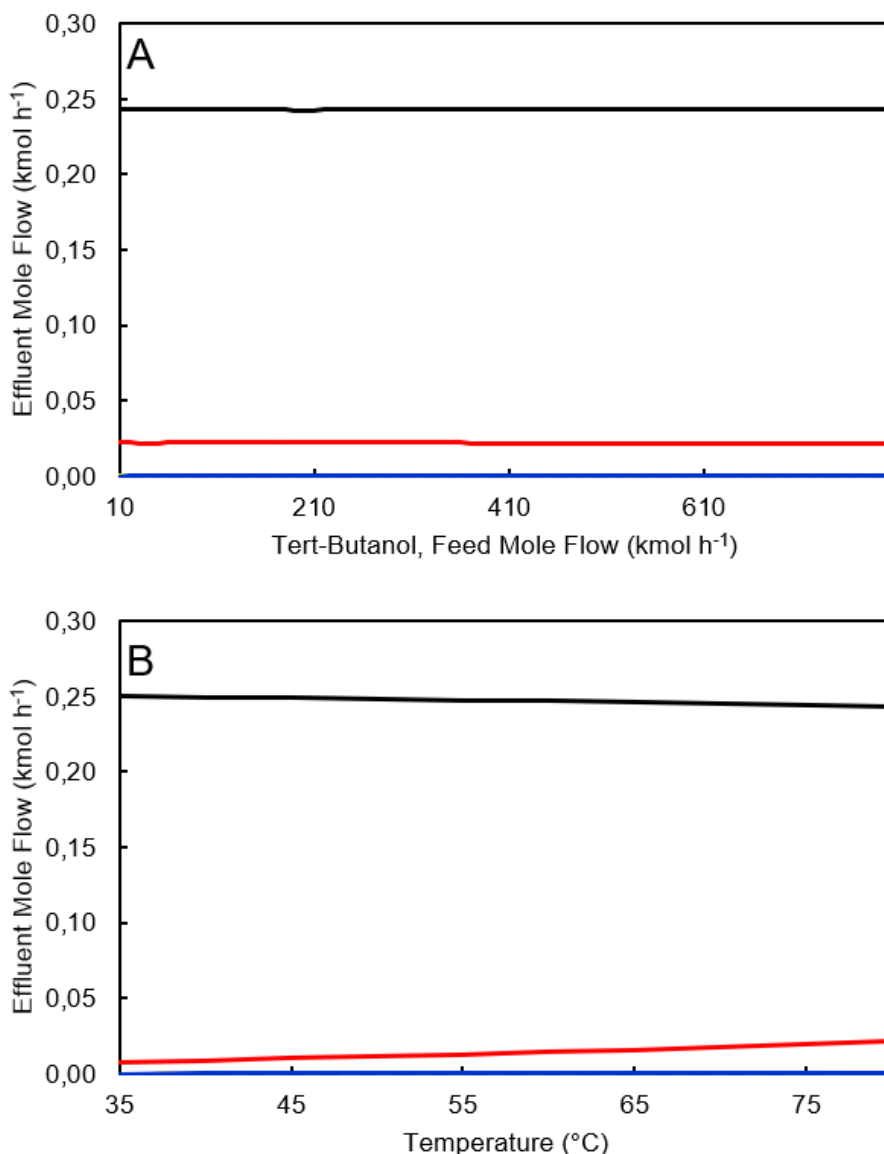


**Figure 6.** Effects on the effluent composition. (A) tert-butanol mole flow in the feed stream and (B) reaction temperature, simulated using Aspen Plus®. Dashed yellow line: TAG; solid black line: DAG; solid red line: MAG, and solid blue line: fatty acid tert-butyl ester. Effluent mole flows of TAG and fatty acid tert-butyl ester are near zero.

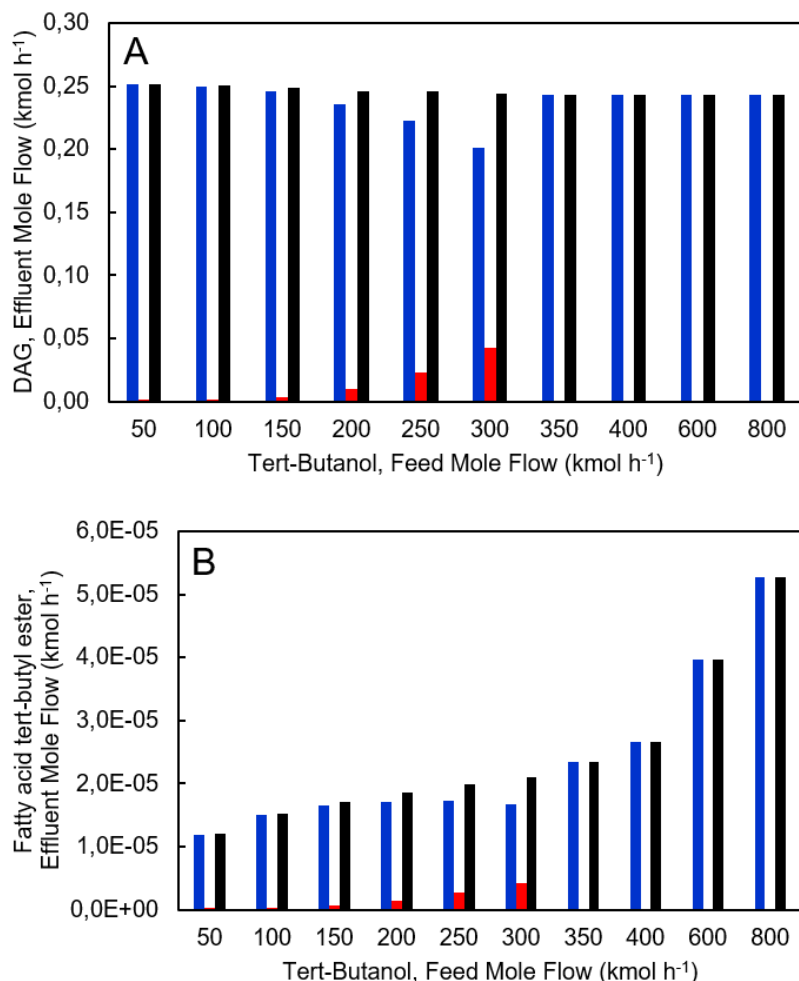


**Figure 7.** Effect of tert-butanol mole flow in the feed stream on the mole flows in the reactor effluent of (A) DAG and (B) fatty acid tert-butyl ester, simulated using Aspen Plus®. Blue bars: L1 (acylglycerols-rich, light-phase); Red bars: L2 (glycerol-rich, heavy-phase); Black bars: L1 + L2 (total amount).

## Conclusion

The UNIQUAC model was well-fitted to the liquid-liquid equilibrium experimental data of systems containing olive oil, glycerol, and C1-C4 alcohols, with *rmsd* values below 1 wt. % for all studied systems. Moreover, the simulation using Aspen Plus® provided an understanding of which products can be thermodynamically preferred when working with glycerolysis of olive oil using glycerol and in the presence of alcohols as solvents. The negligible amount of fatty acid tert-butyl esters predicted in the reactor effluent indicates that tert-butanol may be used as a solvent since thermodynamics indicated this alcohol does not participate in side reactions within the reaction media involved in glycerolysis. Thus, using tert-butanol as a solvent might be interesting and may help to improve the production of a DAG-rich oil.

## Acknowledgments

The authors thank the Brazilian governmental agency CNPq (Research grant 306739/2022-4 and 140168/2024-9) for the financial support and scholarships.

## References

Cabral, P. S., Corazza, M. L., Sasaki, G. L., Grampone, M. A., Irigaray, B. A., & Voll, F. A. P. (2018). Assessment of liquid-liquid phase separation in the composition and oxidation stability of partially hydrolyzed olive oil. *Journal of Food Engineering*, 233, 1–8. <https://doi.org/10.1016/j.jfoodeng.2018.03.025>

Chen, W., Kou, M., Lin, S., & Zhong, N. (2021). Effects of solvents on the glycerolysis performance of the SBA-15 supported lipases. *Journal of Oleo Science*, 70(3), 385–395. <https://doi.org/10.5650/jos.ess20228>

Damstrup, M. L., Abildskov, J., Kiil, S., Jensen, A. D., Sparsø, F. V., & Xu, X. (2006). Evaluation of binary solvent mixtures for efficient monoacylglycerol production by continuous enzymatic glycerolysis. *Journal of Agricultural and Food Chemistry*, 54(19), 7113–7119. <https://doi.org/10.1021/jf061365r>

Damstrup, M. L., Jensen, T., Sparsø, F. V., Kiil, S. Z., Jensen, A. D., & Xu, X. (2005). Solvent optimization for efficient enzymatic monoacylglycerol production based on a glycerolysis reaction. *Journal of the American Oil Chemists' Society*, 82(8), 559–564. <https://doi.org/10.1007/s11746-005-1109-y>

Feltes, M. M. C., de Oliveira, D., Block, J. M., & Ninow, J. L. (2013). The production, benefits, and applications of monoacylglycerols and diacylglycerols of nutritional interest. *Food and Bioprocess Technology*, 6(1), 17–35. <https://doi.org/10.1007/s11947-012-0836-3>

Jin, C., Zhang, X., Geng, Z., Pang, X., Wang, X., Ji, J., Wang, G., & Liu, H. (2019). Effects of various co-solvents on the solubility between blends of soybean oil with either methanol or ethanol. *Fuel*, 244, 461–471. <https://doi.org/10.1016/j.fuel.2019.01.187>

Ke, W., Lee, Y.-Y., Cheng, J., Tan, C.-P., Lai, O.-M., Li, A., Wang, Y., & Zhang, Z. (2024). Physical, textural and crystallization properties of ground nut oil-based diacylglycerols in W/O margarine system. *Food Chemistry*, 433, 137374. <https://doi.org/10.1016/j.foodchem.2023.137374>

Kumoro, A. C. (2012). Experimental and modeling studies of the reaction kinetics of alkaline-catalyzed used frying oil glycerolysis using isopropyl alcohol as a reaction solvent. *Research Journal of Applied Sciences, Engineering and Technology*, 4(8), 869–876.

Li, L., Zhou, Y., Huang, C., Jian, L., Lin, Z., Lin, L., Li, C., & Ye, Y. (2023). Insight into the influence of plant oils on the composition of diacylglycerol fabricated by glycerolysis and esterification. *Industrial Crops and Products*, 204, 117324. <https://doi.org/10.1016/j.indcrop.2023.117324>

Lo, S.-K., Tan, C.-P., Long, K., Yusoff, Mohd. S. A., & Lai, O.-M. (2008). Diacylglycerol oil—Properties, processes and products: A review. *Food and Bioprocess Technology*, 1(3), 223–233. <https://doi.org/10.1007/s11947-007-0049-3>

McNeill, G. P., Shimizu, S., & Yamane, T. (1991). High-yield enzymatic glycerolysis of fats and oils. *Journal of the American Oil Chemists' Society*, 68(1), 1–5. <https://doi.org/10.1007/BF02660298>

Naik, M. K., Naik, S. N., & Mohanty, S. (2014). Enzymatic glycerolysis for conversion of sunflower oil to food based emulsifiers. *Catalysis Today*, 237, 145–149. <https://doi.org/10.1016/j.cattod.2013.11.005>

Nicholson, R. A., & Marangoni, A. G. (2022). Glycerolysis structured oils as natural fat replacements. *Current Opinion in Food Science*, 43, 1–6. <https://doi.org/10.1016/j.cofs.2021.09.002>

Oliveira, H. M., Kanda, L. R. S., Dante, L. Z., Corazza, M. L., Sasaki, G. L., & Voll, F. A. P. (2022). Liquid-liquid equilibrium of systems containing acylglycerols from olive oil, glycerol and isopropanol. *Journal of Chemical Thermodynamics*, 165, 106666. <https://doi.org/10.1016/j.jct.2021.106666>

Rabiah, A., Sebayang, F., & Siahaan, D. (2021). Enzymatic glycerolysis of palm kernel oil using lipase enzyme catalyst from *Candida rugosa* with variations of 1-propanol, 2-propanol, N-heptane, and isoctane solvents. *Journal of Chemical Natural Resources*, 3(1), 2021–2035.

Sandid, A., Spallina, V., & Esteban, J. (2024). Glycerol to value-added chemicals: State of the art and advances in reaction engineering and kinetic modelling. *Fuel Processing Technology*, 253, 108008. <https://doi.org/10.1016/j.fuproc.2023.108008>

Santos, T., Gomes, J. F., & Puna, J. (2018). Liquid-liquid equilibrium for ternary system containing biodiesel, methanol and water. *Journal of Environmental Chemical Engineering*, 6(1), 984–990. <https://doi.org/10.1016/j.jece.2017.12.068>

Singh, A. K., & Mukhopadhyay, M. (2016). Lipase-catalyzed glycerolysis of olive oil in organic solvent medium: Optimization using response surface methodology. *Korean Journal of Chemical Engineering*, 33(4), 1247–1254. <https://doi.org/10.1007/s11814-015-0272-y>

Soares, L. I., Hamerski, F., Basso, H. R., Izidoro Junior, A. M., Koop, L., Corazza, M. L., & Voll, F. A. P. (2018). Liquid-liquid equilibrium of the system glycerolized olive oil + ethanol + glycerol for diacylglycerol enrichment. *Journal of Chemical Thermodynamics*, 124, 38–42. <https://doi.org/10.1016/j.jct.2018.04.020>

Xie, R., Lee, Y.-Y., Xie, P., Tan, C.-P., Wang, Y., & Zhang, Z. (2024). Immobilization of lipase from *Thermomyces lanuginosus* and its glycerolysis ability in diacylglycerol preparation. *Molecules*, 29(17), 4141. <https://doi.org/10.3390/molecules29174141>

Zhong, N., Li, L., Xu, X., Cheong, L., Li, B., Hu, S., & Zhao, X. (2009). An efficient binary solvent mixture for monoacylglycerol synthesis by enzymatic glycerolysis. *JAOCs, Journal of the American Oil Chemists' Society*, 86(8), 783–789. <https://doi.org/10.1007/s11746-009-1402-7>

Zhou, J., Lee, Y.-Y., Mao, Y., Wang, Y., & Zhang, Z. (2022). Future of structured lipids: Enzymatic synthesis and their new applications in food systems. *Foods*, 11(16), 2400. <https://doi.org/10.3390/foods11162400>